Published in final edited form as:
Biochemistry. 2007 November 13; 46(45): 12968–12978. doi:10.1021/bi701525w.

Serum Opacity Factor Unmasks Human Plasma High-Density Lipoprotein Instability via Selective Delipidation and Apolipoprotein A-I Desorption†

Baiba K. Gillard[‡], **Harry S. Courtney**[§], **John B. Massey**[‡], and **Henry J. Pownall**[*,‡]

[‡]Section of Atherosclerosis and Vascular Medicine, Department of Medicine, Baylor College of Medicine, Houston, Texas 77030

[§]Veterans Affairs Medical Center and Department of Medicine, University of Tennessee Health Science Center, Memphis, Tennessee 38104

Abstract

Human plasma high-density lipoproteins (HDL) are important vehicles in reverse cholesterol transport, the cardioprotective mechanism by which peripheral tissue-cholesterol is transported to the liver for disposal. HDL is the target of serum opacity factor (SOF), a substance produced by *Streptococcus pyogenes* that turns mammalian serum cloudy. Using a recombinant (r) SOF, we studied opacification and its mechanism. rSOF catalyzes the partial disproportionation of HDL into a cholesteryl ester-rich microemulsion (CERM) and a new HDL-like particle, neo HDL, with the concomitant release of lipid-free (LF)-apo A-I. Opacification is unique; rSOF transfers apo E and nearly all neutral lipids of ~100,-000 HDL particles into a single large CERM whose size increases with HDL-CE content (r ~100–250 nm) leaving a neo HDL that is enriched in PL (41%) and protein (48%), especially apo A-II. rSOF is potent; within 30 min at 37 °C, 10 nM rSOF opacifies 4 μM HDL. At respective low and high physiological HDL concentrations, LF-apo A-I is monomeric and tetrameric. CERM formation and apo A-I release have similar kinetics suggesting parallel or rapid sequential steps. According to the reaction products and kinetics, rSOF is a heterodivalent fusogenic protein that uses a docking site to displace apo A-I and bind to exposed CE surfaces on HDL; the resulting rSOF–HDL complex recruits additional HDL with its binding-delipidation site and through multiple fusion steps forms a CERM. rSOF may be a clinically useful and novel modality for improving reverse cholesterol transport. With apo E and a high CE content, CERM could transfer large amounts of cholesterol to the liver for disposal via the LDL receptor; neo HDL is likely a better acceptor of cellular cholesterol than HDL; LF-apo A-I could enhance efflux via the ATP-binding casette transporter ABCA1.

High-density lipoproteins, the primary plasma vehicle for reverse cholesterol transport (RCT[1]), occur in buoyant and dense forms, HDL_2 and HDL_3, and comprise free cholesterol (FC), cholesteryl esters (CE), phospholipids (PL), small amounts of triglyceride (TG), and

†This work was supported by grants-in-aid from the National Institutes of Health (HL-30914 and HL-56865 to H.J.P.) and by research funds from the Department of Veterans Affairs (to H.S.C.).

*Corresponding author. Baylor College of Medicine, One Baylor Plaza, MS A601, Houston, TX 77030. Phone: (713) 798-4160. Fax: (713) 798-9005. hpownall@bcm.tmc.edu.

[1]Abbreviations: apo, apolipoprotein; LF, lipid-free; rSOF, recombinant serum opacity factor; HDL, LDL, and VLDL, high, low, and very low density lipoproteins, respectively; TG, triglyceride; PL, phospholipid; CE, cholesteryl ester; LCAT, lecithin:cholesterol acyltransferase; SEC, size exclusion chromatography; RCT, reverse cholesterol transport; SR-BI, scavenger receptor class B, type I; TBS, trisbuffered saline.

apolipoproteins (apos), mainly apos A-I, A-II, C, and E (1–3). All HDL components exchange by spontaneous (4) or protein-mediated mechanisms (5,6). HDL is an unstable particle residing in a kinetic trap from which it can escape by chaotropic (7), detergent (8), or thermal perturbation (7,9). HDL instability is subfraction-specific with the larger fractions including HDL_2 being more stable than the smaller HDL_3 (10). Release of lipid-free (LF)-apo A-I in response to physicochemical perturbations, which is a hallmark of HDL instability (7–10), is important in two physiological contexts. First, the initiating step in RCT, cellular cholesterol efflux, occurs through the interaction of lipid-free (LF)-apo A-I with an ATP-binding cassette (ABC)A1 transporter (11). Second, the terminal step in RCT, selective removal of HDL-cholesteryl ester via the hepatic HDL receptor scavenger receptor class B, type I (SR-BI), excludes apo A-I (12,13), a process that occurs via a delipidation step for which the molecular mechanism is not known.

Serum opacity factor (SOF) is a substance produced by *Streptococcus pyogenes* that turns mammalian serum opaque (14). SOF is a virulence determinant expressed by approximately half of the clinical isolates of *S. pyogenes*, a human pathogen that causes a wide spectrum of diseases ranging from pharyngitis to overwhelming invasive infections with high rates of morbidity and mortality (15). The target of opacification is HDL; other lipoproteins are not substantively affected. rSOF opacifies HDL without breaking covalent bonds and is neither a protease nor a lipase (16). The products of SOF activity are buoyant lipid droplets that are devoid of apos and a denser fraction that is rich in apos A-I and A-II. SOF appears to interact with HDL-aposA-I and A-II, thereby triggering the extrusion of HDL lipids, which coalesce into lipid droplets whose growth produces opacification (16). Identification of the mechanism by which any substance or process selectively delipidates HDL is of interest because the accruing insights may help identify new therapeutic modalities. Given its unusual activity and specificity against human plasma HDL, we have investigated the nature of the rSOF reaction against HDL, the structures and qualities of the products, and the mechanism by which they form.

MATERIALS AND METHODS

Materials

1-Palmitoyl-2-oleoyl phosphatidylcholine (POPC) was from Avanti Polar Lipids. HDL was isolated according to its density by sequential flotation of human plasma obtained from The Methodist Hospital Blood Donor Center. The HDL subfractions were separated by SEC in which increasing elution volume (E_V) corresponds to decreasing particle size. Fractions from multiple injections (0.5 mL) were pooled and concentrated as needed by placing the sample in a dialysis sack (12,000–14,000 MW exclusion) and placing Sephedex G75 on the outside to remove water. Alternatively, HDL (330 mg) was separated into 10 fractions by ultracentrifugation in a density gradient between 1.11 and 1.17 g/mL created with KBr. Four fractions, HDL_2 and buoyant (B), intermediate (I), and dense (D) HDL_3 with respective densities of ≤1.11, 1.13, 1.15 and ≥1.17 g/mL were selected for testing with SOF. A polyhistidine-tagged, truncated form of *sof2* encoding amino acids 38–843 was cloned and expressed in *Escherichia coli* (rSOF) and purified by metal affinity chromatography as described previously (16). The effect of SOF on HDL and the generation of large CERM particles has been noted with both native and recombinant poly histidine-tagged SOF, indicating that the histidine tag did not alter the biological activity of SOF (data not shown). Apolipoprotein compositions were determined by SDS–PAGE using 15% Tris-Glycine Ready Gels (Bio-Rad). Bands were visualized with Pierce GelCode Blue stain reagent, destained, and recorded by photography. The apo A-I and apo A-II contents of the HDL subfractions were not remarkably different (data not shown).

Biological Labeling of HDL with [^{3}H]CE

[^{3}H]Cholesterol (0.1 mCi) was dried under vacuum and redissolved in 100 μL of 95% ethanol. HDL (2 mL, 9.6 mg/mL) was combined with the lecithin:cholesterol acyltransferase (LCAT) activity from the clear zone obtained from the flotation of HDL (4-mL), and the ethanolic solution was added dropwise while stirring and incubated at 37 °C with mild agitation. Conversion of FC to CE was followed by removing 100 μL at various times, extracting into hexane, and measuring CE formation by TLC. To remove unreacted free cholesterol, the HDL was mixed with LDL (5 mL 5.8 mg/mL) and incubated for 3 h at 37 °C. At the end of the incubation, the density was adjusted to 1.063 g/mL and the LDL floated and removed. The labeled HDL was adjusted to d = 1.21 g/mL by the addition of KBr and the [^{3}H]CE-labeled HDL_3 (0.8 μCi/mg protein) isolated by flotation. According to liquid scintillation counting of spots collected after thin layer chromatography, 97% of the radioactivity eluted as CE. The SEC profile of HDL absorbance at 280 nm and [^{3}H]CE radioactivity were nearly the same. [^{3}H]HDL was separated into six fractions by SEC and analyzed by SEC before and after incubation with rSOF.

Analysis of rSOF Activity by SEC

Various amounts of HDL and rSOF were combined at 37 °C. At the end of each incubation, an aliquot (0.2 mL) was analyzed by SEC using an Amersham-Pharmacia ÄKTA chromatography system equipped with two Superose HR6 columns in tandem and eluted with TBS at a flow rate of 0.45 mL/min. The column effluent was monitored by absorbance (280 nm) and the radioactivity of collected fractions. Stoke's radii were calculated from a calibration curve based on protein standards of known Stoke's radius (r). A Stoke's volume (V_S) was calculated as $V_S = 4/3\pi r^3$.

Composition of rSOF-HDL Products

HDL (0.5 and 21 mg/mL, respectively) were incubated for 24 h with rSOF (1 and 4 μg/mL) at 37 °C. For preparative chromatography in which the effluent was collected for analysis, a 0.5 mL sample loop was used; pooled fractions from multiple runs were analyzed for protein using a commercial kit (BioRad DC Protein Assay) and for cholesterol, cholesteryl ester, triglyceride, and PC, using commercial kits (Wako Chemicals, Inc. Richmond, VA). Apoprotein composition was determined by SDS–PAGE using 4–15% gradient or 18% Tris-Glycine Ready gels (BioRad). Bands were visualized with Pierce GelCode Blue stain reagent, destained, and recorded with the Kodak Electrophoresis Documentation and Analysis System (EDAS 290).

Western Blots

SEC fractions were analyzed for apos and SOF by Western blotting. Proteins were resolved on 15% Tris-Glycine Ready Gels (BioRad) by SDS–PAGE and transferred to nitrocellulose for immunoblotting. The Western blotting method was essentially that of the Amersham ECL-plus manual (Amersham GE Healthcare). Immunoblots were conducted with HRP-conjugated goat anti-human apo A-II, apo E, apo A-I, and apo B from Academy Biomedical (Houston, TX). Titration of standard apos gave detection limits of less than 0.1 ng for the three HDL apos A-I, A-II and E. Both the anti-apo E and anti apo A-II detected the apo A-II-E heterodimer. However, relative exposure times indicated that the anti apo E antibody was about 150 times more sensitive than was the anti-apo A-II antibody. Anti-SOF was a rabbit antiserum to rSOF2ΔFn (16) and was detected with an HRP-conjugated goat anti-rabbit IgG second antibody (BioRad).

RESULTS

Compositions of the Products of rSOF and HDL

HDL (0.5 mg/mL) elutes from a SEC column as a single peak with an elution volume corresponding to a molecular volume of ~ 670 nm^3. After incubation of HDL (0.5 mg/mL) and rSOF (1 μg/mL) for 24 h at 37 °C, the initially clear HDL solution was translucent. The products were separated by SEC, and the collected fractions analyzed (Figure 1; Table 1). The fraction appearing in the void volume contained ~60% of the total CE that eluted from the column, 4% of the PL, and only ~1% of the protein. This fraction is rich in neutral lipids (NL ~73%), particularly CE (Table 1); accordingly, we refer to the particles in this fraction as cholesteryl ester-rich microemulsion (CERM). Another new HDL-like particle eluting slightly later than HDL contained 87% of the PL applied to the column, ~60% of the protein ~75% of the TG, and ~80% of the free cholesterol. Protein and PL accounted for nearly 90% of its composition; according to its composition and size (Table 1), we called the particles in this fraction neo HDL; relative to HDL, neo HDL is PL- and apo A-II-rich (Figure 1D and F; Table 1) and one-third smaller (~450 nm^3). Calculation of the stoichiometry of CE, TG, and PL in HDL and neo HDL shows that the number of CE molecules per particle is reduced by rSOF but that PL content is conserved (Table 1). Immunoblot analysis revealed the presence of apo E in the leading edge of the neo HDL (Figure 1F). The last peak to elute from the column was lipid-free and had an elution volume identical to that of an authentic sample of apo A-I, which has a measured Stoke's volume of ~230 nm^3 (Figure 1E); immunoblot analysis showed that this peak contained apo A-I but no apo A-II (Figure 1F). Thus, this fraction is lipid-free (LF)-apo A-I.

Similar studies at higher concentrations of HDL and rSOF permitted the visualization of low abundance components and revealed a change in the state of association of LF-apo A-I. Incubation of rSOF (4 μg/mL) with HDL (21 mg/mL; 24 h, 37 °C) rendered the clear yellow HDL solution totally opaque. Both CERM and neo HDL appeared in the SEC and had compositions similar to those observed at low HDL concentrations (Figure 2; Table 1). The CERM contained ~80% of the total CE in the reaction products. The corresponding values for the other components decreased in the order TG (43%) > FC (38%) > PL (8%) > protein (0.5%). The protein profiles obtained by chemical analysis and quantitative immunoblot analysis of apos A-I and A-II were nearly identical (Figure 2E) so that the SEC apo distribution can be assigned with confidence. These showed coelution of all apo A-II but not apo A-I with the neo HDL (Figure 2F). Immunoblotting also revealed the occurrence of apo E in the CERM and in the larger neo HDL particles (Figure 2G). Apo E was also prominent on larger particles that eluted later than the void volume (22–25 mL). We speculated that these are intermediates destined to become CERM. At these higher reactant concentrations, rSOF was observed in the CERM and as a possible ~50 kDa fragment in neo HDL; this was consistently observed and may be due to proteolysis during the long (24 h) incubation. Finally, in contrast to the monomeric LF-apo A-I found at low reactant concentrations, at high concentrations, a shoulder and peak eluting at ~26 and ~28 mL were practically lipid-free. These particles were ~1800 and ~790 nm^3, respectively; lipid and immunoblot analysis showed the protein to be mostly lipid-free apo A-I (Figure 2G boxed) with a trace of apo E that is likely the overlapping edges of peaks for neo HDL and earlier eluting species. On the basis of their respective elution volumes, these particles are apo A-I octamers and tetramers.

Effect of rSOF Concentration

HDL (0.25 mg/mL) was incubated with various concentrations of rSOF for 0.5 h at 37 °C. As the rSOF concentration was increased from 0.1 to 20 μg/mL, the starting HDL SEC profile gradually shifted to the smaller neo HDL with a simultaneous increase in the magnitude of the peak for LF-apo A-I (Figure 3A). Over the same rSOF concentration range, the peak elution

volume for the CERM shifted from the void volume (14.7 mL) at 0.1 μg/mL rSOF into the included volume as the rSOF concentration was increased (Figure 3A and B); at 20 μg/mL rSOF, the absorbance peak for the CERM appeared at 15.1 mL. The SEC are reproducible; the elution volume of the CERM from multiple injections (n = 14) was 15.00 ± 0.0157 (SE). Thus, the sizes of the particles that comprise the CERM decrease with increasing rSOF concentration. Consistent with the production of smaller particles, the absorbance due to opacification decreased as the rSOF concentration was raised from 0.3 to 20 μg/mL (Figure 3B).

Effect of HDL Concentration on the Opacification Reaction

The effect of HDL concentration on opacification by rSOF was also assessed. At low concentrations, HDL eluted as a single broad peak (Figure 4A) that was replaced by CERM, neo HDL, and LF-apo A-I after incubation with rSOF at 37 °C for 3 or 22 h. Between 1 and 10 mg/mL HDL, the magnitude of the peak for the CERM grew, while a new peak appeared, first as a shoulder at 2 mg/mL HDL and then at higher concentrations as a prominent peak at ~28 mL (marked by asterisks in Figure 4B–E); the magnitudes of this peak, identified as LF-apo A-I oligomers (Figure 2), and the peak in the void volume were higher after 22 h. Thus, rSOF converts HDL to CERM and apo A-I oligomers in a concentration- and time-dependent way.

Speciation of rSOF Activity

Analysis of the effects of rSOF on HDL subfractions separated according to size showed major differences in the SEC profiles, particularly the amount of material in the void volume (Figure 5). As expected, chemical analysis of the fractions showed that the NL content of the HDL subfractions increased with increasing particle size (Table 2). The amount of material eluting in the void volume, based on integrated absorbance, increased with increasing particle size (Figure 5B–F) and was highly correlated with the sum of the NL (CE + TG) content of the starting HDL particles (Figure 5G; r^2 = 0.82). Incubation of rSOF with all HDL subfractions gave rise to a neo HDL with essentially the same particle size. Similar effects were observed with HDL isolated according to density with the SEC profiles of the larger HDL_2 after incubation with rSOF being similar to that of the largest HDL fraction isolated by SEC and the corresponding HDL_3 profile being similar to those of the smaller SEC HDL fractions (data not shown).

[^{3}H]CE-labeled HDL was used to follow the redistribution of HDL-CE into CERM and neo HDL. [^{3}H]CE-labeled HDL separated into six fractions by SEC (data not shown), which were analyzed by SEC before and after incubation with rSOF. According to the SEC absorbance profiles, rSOF converted all subfractions into CERM, LF-apo A-I, and neo HDL, and with decreasing HDL size, the fraction of HDL-protein converted to neo HDL increased, while the amount of LF-apo A-I formed was constant (Figure 6 B). The isosbestic point at ~31 mL is suggestive of a simple two-state system, HDL and neo HDL, with the amount of LF-apo A-I, the a third component formed, being constant across all fractions. The absorbance and HDL-[^{3}H]CE profiles of each starting subfraction were nearly co-incident (Figure 6A and C). The product profile as assessed by HDL-[^{3}H]CE radioactivity was similar to that for absorbance except for the absence of the peak for LF-apo A-I (Figure 6B and D). Despite the profound shift in the HDL-[^{3}H]CE profile of neo HDL with decreasing HDL size (Figure 6D, compare black and red curves), the fraction of [^{3}H]CE in neo HDL declined with decreasing size. Also, the fraction of [^{3}H]CE in neo HDL decreases with decreasing size of the HDL from which it is derived (Figure 6D, insert). These data corroborate the compositional data (Figures 1 and 2) on the distribution of HDL-CE and show that our labeling method gives a product for which the distribution of [^{3}H]CE is similar to that of chemically determined CE. Moreover, these data show that rSOF releases the same amount of LF-apo A-I from all HDL subfractions but that

the smaller more protein-rich subfractions that contain less PL form neo HDL that have less CE.

Kinetics of HDL Opacification

rSOF was incubated with HDL-[^{3}H]CE and the redistribution of absorbance and [^{3}H]-CE was followed with time by SEC. Before incubation, SEC analysis showed the coelution of protein absorbance and radiolabel (Figure 7A and B, black curves). Following the addition of rSOF to HDL, the magnitude of the peak absorbances for CERM, neo HDL, and LF-apo A-I rose, while that for HDL fell. Although not apparent in the absorbance profile, with a 10-fold amplification, the radio-label analysis reveals the early appearance of CE in fractions between the CERM and the neo HDL that level off at $t > 85$ min (Figure 7B insert). On the basis of the rate of increase in the peak for LF-apo A-I, a first-order rate constant was calculated as $k_{AI} = (2.1 \pm 0.006) \times 10^{-2}$ min^{-1} ($r^2 > 0.96$). The rate constant for the formation of CERM, calculated from the rate of transfer of HDL-associated [^{3}H]CE to CERM was $k_{CERM} = (3.2 \pm 0.008) \times 10^{-2}$ ($r^2 > 0.99$). Additional rSOF (1 μg/mL) and incubation for another 7 h did not change the final elution profile. Given that $k_{AI} \approx k_{CERM}$, CERM formation and release of LF-apo A-I are either concerted processes or occur in rapid succession. As expected, the reaction rates increase with temperature and yield linear Arrhenius plots between 25 and 42 °C (data not shown).

rSOF Does Not Displace Apo A-I from Superphospholipidated (SPLd) HDL

Given that PL are the essential apo-associating components of HDL, we tested whether increased HDL-PL would stabilize HDL against rSOF. Using a modified detergent dilution method (8), the PL content of HDL was increased by the addition of POPC. Relative to control HDL-PL = 100, the PL contents of the SPLd species were 100 ± 0.2, 152 ± 0.05, 245 ± 0.06, and 393 ± 0.01. According to SEC analysis, SPLd HDL were slightly larger than HDL; this was confirmed by nondenaturing gradient gel electrophoresis, which showed a shift in HDL particle mass from ~150 to ~350 kDa (data not shown). As expected, incubation of HDL (0.8 mg/mL) with rSOF (1 μg/mL) produced CERM, neo HDL, and LF-apo A-I (Figure 8). Similar incubations with SPLd containing 1.5-fold HDL-PL reduced the amount of neo HDL formed and LF-Apo A-I released (Figure 8B), and SPLd HDL containing more than 1.5 fold HDL-PL formed even less neo HDL and released no LF-apo A-I. Thus, the addition of PL partially stabilizes HDL against CERM formation and especially the release of LF-apo A-I (Figure 8A–C). The increase in the void volume peak (Figure 8D) in the presence of 4-fold HDL-PL is likely due to a small amount of CERM superimposed on PL multilayers (17).

Apo A-I Self-Associates at Physiological Concentrations

Apo A-I at various concentrations was analyzed by SEC (data not shown). At 0.1 and 0.3 mg/mL, apo A-I elutes as a single peak (E_V ~34 mL; Stoke's volume = 230 nm^3). As the concentration increased to 5 mg/mL, the E_V shifted to ~29.5 mL (Stoke's volume = 864 nm^3), which corresponds to tetrameric apo A-I. In each case, the injected 0.2 mL was diluted to at least 2 mL by the chromatography so that the concentration at which apo A-I self-association occurs is 10% of that injected, that is, >0.03 mg/mL. Thus, apo A-I forms higher order oligomers in a concentration-dependent way and is monomeric only at injected apo A-I concentrations ≤0.3 mg/mL, which corresponds to an eluted concentration of ≤0.03 mg/mL.

DISCUSSION

Opacification Reaction

rSOF selectively delipidates HDL via a limited HDL disproportionation, that is, partial segregation of HDL lipids and proteins to form three major products, CERM, neo HDL, and LF-apo A-I. At reaction completion, neo HDL contain most of the PL and protein, with the

remainder of the protein occurring as LF-apo A-I. On the basis of changes in composition, each neo HDL is derived from a single HDL, which is 19.8% CE and 47.3% protein (Table 1). According to the tabular data that was used to create Figure 1A and E, rSOF transfers 90% of the HDL-CE to the CERM and converts 40% of the protein to LF-apo A-I, thereby reducing the particle volume by (0.9 × 19.8% ≈ 18) + (0.4 × 47.3% ≈ 19%) = 37%, leaving a particle that has 63% of the mass of the starting HDL. This value compares favorably with the ratios of the volumes of neo HDL and HDL measured by SEC (100% × 450 nm^3/650 nm^3 = 69%) and is thus consistent with each neo HDL being derived from a single HDL. This conclusion is supported by stoichiometric considerations. According to its mass (125 kDa) and composition, each HDL contains 38, 6, and 44 CE, TG, and PL molecules, respectively, compared to 80 kDa, 4, 6, and 44, respectively, for neo HDL (Table 1). Thus, the number of PL molecules per particle is conserved during opacification (Table 1). NL give lipoproteins their spheroidal shape through phase separation into a central core. Neo HDL contains only 4 and 6 CE and TG per particle, respectively. Phase separation occurs when the CE and TG content exceeds 3 mol % of PL (18). For neo HDL, this corresponds to 1 molecule of each leaving 3 CE and 5 TG molecules, respectively, per neo HDL particle. Theoretically, this would be high enough to produce segregation into a lipid lens but would not give rise to a prominent core so that neo HDL is likely discoidal.

The CERM are spherical particles with sizes ($r \approx 250$ nm) and NL composition (~80%; Table 1) comparable to those of chylomicrons, the largest plasma lipoproteins (1). Unlike chylomicrons, CERM is CE-rich, making it the largest known CE-containing lipoprotein formed by a physiological reaction. In contrast to neo HDL, which are derived from a single HDL particle, many HDL contribute CE to CERM; these large particles (r) 150–250 nm) have calculated volumes $V \sim(1 – 60) \times 10^7$ nm^3 so that each CERM contains the CE equivalent of >100,000 HDL particles! Intact rSOF is only found in the CERM (Figure 2G). In contrast, an immunoreactive band with a mass of 50 kDa may be a fragment formed by an HDL-associated protease.

Thermodynamics of Opacification

The thermodynamics of the rSOF-mediated delipidation of HDL can be rationalized in the context of the principle-of-opposing-forces model of Tanford (19). In the absence of amphiphiles, NL in water form a single phase that is stabilized by hydrophobic forces. In the presence of amphiphiles, such as PL and to a lesser extent apos, a second force comes into play, that is, the tendency of amphiphilic components to associate in ways that bury their hydrophobic surfaces but leave their polar or charged moieties available for high energy solvation by water. For PL, the hydrophobic surface is defined by their acyl chains, and the solvation site is their zwitterionic headgroups; for apos, the hydrophobic surface is the nonpolar face of their amphipathic helices, and the polar sites are on the opposing helical surfaces that contain polar and charged amino acid residues. The balance of these two forces, determined by the physical properties of the reactant components, their relative abundance, and the attendant mechanisms, which may follow different reaction coordinates, determines the product profile, which lies somewhere between total phase separation and total homogeneity.

Given that opacification is spontaneous, the free energy of the reactants must be higher than those of the products, which must be stabilized by more favorable intermolecular forces. rSOF transfers most of the lipid components of HDL to the CERM, leaving the balance of the lipid components with neo HDL. The exception, LF-apo A-I, is notable because it is the least lipophilic of all the components of HDL so that in the competition for the limited amount of PL in CERM and neo HDL, some apo A-I is excluded from both macromolecular species. Thus, one of the effects of rSOF is to remove low affinity apo A-I from HDL while leaving the higher affinity apo A-II, an effect that is emulated by chaotropic perturbation (10).

However, in the presence of adequate phospholipid, HDL-apo A-I is stabilized, and apo A-I is not released (Figure 8). Thus, phospholipid is essential to HDL stability, and physiological activities that consume or transfer phospholipid, LCAT, hepatic lipase, cholesteryl ester transfer protein, and phospholipid transfer protein, would destabilize HDL-apo A-I (20–24). The greater lability of apo A-I can also be inferred from human studies showing that the fractional catabolic rate of apo A-I in normolipidemic and hypo α-lipoproteinemic patients is greater than that of apo A-II (25), presumably through greater renal loss of LF-apo A-I (13).

The rSOF-mediated redistribution of apo E and rSOF is distinct from those of apos A-I and A-II. At low HDL concentration, apo E–apo A-II heterodimers are associated with the large HDL subfractions, one of which contains only a trace of dimeric apo A-II but no apo A-I (Figure 1F, fraction 31). Higher reactant concentrations reveal apo E as monomers, homodimers, and heterodimers with apo A-II (Figure 2G). Relative to the small neo HDL, which is rich in homo and heterodimers, in large neo HDL (fractions 22–26) apo E monomers and heterodimers predominate. Although chemical analyses showed little or no lipid in fractions 22–26 (Figure 2), reaction of rSOF with HDL labeled with [^{3}H]CE (Figure 7B, insert), shows increasing CE in this elution range at longer incubation times. Thus, like apo A-II, apo E is always observed as a lipidated species. Within the CERM fraction, monomeric apo E predominates.

Apo A-I Self-Association

Although a well-known phenomenon (25,26), the relevance of apo A-I self-association to a physiological context has never been established. We show for the first time a reaction in which concentration-dependent apo A-I self-association determines a product profile under physiological conditions. Our data (Figures 2 and 4) show clear evidence of apo A-I oligomerization within the typical human plasma HDL protein concentration range of ~1.5–2 mg/mL (1). Moreover, the oligomeric state corresponds to the apo A-I tetramers that have been identified by hydrodynamic methods (26).

Speciated HDL Opacification

Our data showed that the neo HDL formed from the smaller HDL species are smaller than those formed from the largest HDL (Figure 5 B–F) and that CERM formation is a linear function of HDL-NL content (Figure 5G). Interestingly, the amount of LF-apo A-I is constant across a range of HDL sizes, whereas the amount of neo HDL formed increases with decreasing size of the starting HDL (Figure 6B). These data are consistent with the formation of one neo HDL of fixed composition from each HDL particle. At constant HDL-protein concentration, there are fewer large particles; therefore, fewer neo HDL form for the same amount of LF-apo A-I. Although rSOF transfers most of the CE to CERM, a small amount appears in neo HDL (Figure 6D). This reflects the sparing solubility of CE in PL (18) and the PL-rich nature of neo HDL. Consistent with this, the percentage of CE in neo HDL decreases with decreasing size and PL content (Table 2) of the HDL from which it was derived. Moreover, the higher amount of TG than CE in neo HDL reflects its higher solubility in PL (18). Thus, rSOF removes CE from the HDL core but leaves a small fraction that is solubilized by the PL.

A Mechanistic Model for Opacification

rSOF is catalytic; without being consumed, 1 μg/mL (~10 nM) rSOF opacifies 1000 molar excess of HDL (1 mg/mL = 10 μM) and in the process transfers a >40,000 molar excess of CE to CERM. Thus, any mechanistic model would have to account for a highly efficient process in which rSOF catalyzes the opacification of 400 to >3000 molar excess of HDL (Figures 1 and 2) and for kinetics that are exponential with respect to CERM growth and LF-A-I release.

We considered two mechanistic models. In the first, which is similar to the carrier mechanism for lipid transfer by CE-transfer protein (27), rSOF transfers one or more CE particles from

one HDL to another that eventually grows to a CERM through successive transfer cycles. This mechanism was rejected for several reasons. Its efficiency would be reduced by reversibility; only a limited number of CE could be carried per cycle; this mechanism would require distinct binding determinants on rSOF that would direct rSOF to HDL and the rSOF-CE complex to the growing CERM; in the absence of those determinants that define specificity, rSOF would collide much less frequently with CERM particles than with HDL particles whose numbers exceed those of the growing CERM particle by a factor of ~100,000; the isosbestic point in the SEC kinetic analysis suggests a simple two-state system; and finally, this model would not account for exclusive association of rSOF with CERM (Figure 2G).

Our alternative mechanistic model is that rSOF is a heterodivalent fusogenic protein that binds to exposed CE surfaces that are formed by the desorption of apo A-I and recruits additional HDL-CE in multiple steps (Figure 9). Step 1: rSOF binds to an HDL particle with its high affinity docking site (HDS) and displaces apo A-I, thereby forming the HDL host–rSOF complex that is destined to become a CERM. This could occur through rSOF insertion into the surface monolayer of HDL, thereby raising the surface pressure and displacing the most weakly associated component, apo A-I, into the aqueous phase. Alternatively, spontaneous desorption of apo A-I into the aqueous phase could free up transient hydrophobic CE patches on the surface of HDL that are sites of rSOF-HDS insertion and docking. The surface association of rSOF is supported by our data (Figure 3) and previous studies (16), showing that as the amount of rSOF increases, the size of CERM decreases, thereby providing a greater amount of total surface to accommodate an increasing number of rSOF molecules. A second guest HDL particle diffuses to the low affinity delipidation site (DS) of rSOF. Step 2: a transient guest–host complex forms, and a continuous stalk joins the neutral lipid cores of the two HDL . Step 3: CE in the guest HDL particles transfers to and coalesces with those of the host HDL, and the neo HDL is extruded into the aqueous phase; this step, CE partitioning into one compartment, would be expected to provide some of the free energy that drives the reaction. Although most alternative models would require divalancy, that is, two HDL binding sites on rSOF, it is the irreversibility of the reaction and CERM growth that requires heterodivalency because in a homodivalent system, CE could flow from guest to host or host to guest. Step 4 comprises multiple cycles of host–guest interactions that ultimately form (Step 5) numerous neo HDL and CERM that contains rSOF and apo E as the only detectable proteins. Notably, the immunoblotting data (Figure 2G) shows that the CE-containing particles eluting between the mature CERM and HDL (Figure 7B) are more apo E-rich than the CERM. We speculate that this is due to the much greater total surface area and attendant higher surface content of PL, which mediates apo E binding.

This model is consistent with our kinetic data (Figure 7). Under our kinetic conditions, HDL (125 kDa at 0.5 g/L; [HDL] = 4×10^{-6} M) and rSOF (100 kDa at ~1 mg/L; [rSOF] = 10^{-8} M) and the diffusion-controlled rate constant $k_d = 3 \times 10^{11}$ M^{-1}- min^{-1}. The initial step is the diffusion-controlled formation of the HDL–rSOF complex according to the following equation:

$$\mathrm{HDL + rSOF} \rightarrow \mathrm{HDL - rSOF} \quad (1)$$

This is followed by the multiple fusion reactions that form the growing CERM as given by the following equation:

$$\mathrm{HDL - rSOF + HDL} \rightarrow \mathrm{CERM} \quad (2)$$

The concentration of the rSOF–HDL complex is equal to that of rSOF so that

$$\text{rate} = k_d[\text{rSOF} - \text{HDL}][\text{HDL}] = 3 \times 10^{11}\text{M}^{-1} - \text{min}^{-1} \times 4 \times 10^{-6}\text{M} \times 10^{-8}\text{M} \quad (3)$$

Given that first-order kinetics were observed and that HDL is in great excess, eq 3 gives a pseudo first-order rate of ~1×10^{-2} min^{-1}, which corresponds well with the observed values of $k_{CERM} = (3.2 \pm 0.008) \times 10^{-2}$ and $k_{AI} = (2.1 \pm 0.006) \times 10^{-2}$ min^{-1}.

According to our model, one would expect some remnant apos A-I and A-II that resided in the host HDL to be found in the mature CERM product. This was not observed for two possible reasons. Given that one host HDL accommodates 100,000 guest HDL, the amount remaining in the CERM may be below our detection limit. Alternatively, and more likely, apo A-I and A-II have a low affinity for CERM and at some point in its growth desorb into the aqueous phase. Although our model shows interaction of rSOF with a surface CE patch as an important step in opacification, the formation of LF-apo A-I determines specificity for HDL. VLDL and LDL are not appreciably opacified by rSOF (16). Whereas, VLDL is relatively low in CE, LDL has a high CE content. However, neither contains apo A-I, the labile component of HDL (7−9).

The desorption of apo A-I from HDL is a hallmark of its instability as revealed by both physicochemical (7−10) and physiological perturbants (20−24), some of which also produce CERM (7,10). However, not even chaotropic perturbation with 6 M guanidinium chloride produces as much of the CERM so that the rSOF reaction against HDL is unusual if not unique and unprecedented for a water-soluble protein. Two proteins have activities that share some characteristics with rSOF. One is microsomal transfer protein MTP-A, which catalyzes the coalescence of CE- and TG-rich particles during hepatic VLDL assembly (28). Within adipocytes, MTP-B, a splicing variant of the canonical MTP-A, appears to catalyze the fusion of small TG-rich inclusions into large ones (29). The other protein, SR-BI, is an HDL receptor, which mediates net cellular internalization of HDL-lipids, especially CE. Similar to rSOF, SR-BI selectively removes CE from HDL at the cell surface while excluding apo A-I from net uptake (12,13).

Clinical Relevance

One of the remaining plasma lipo-protein risk factors for which current therapies are inadequate is low HDL cholesterol and its attendant dysregulated RCT. HDL opacification is a potential therapeutic modality for improving RCT because it rapidly transfers HDL-CE to a particle that contains apo E, a ligand for the hepatic LDL receptor, which could remove large amounts of HDL-derived CE. At the same time, neo HDL, which is CE-poor, is available to initiate additional cycles of cellular cholesterol efflux, esterification, opacification, and removal. SOF opacification could produce a potentially detrimental state: low HDL-C. However, studies in mice in which SR-BI has been ablated or overexpressed suggest that more efficient RCT due to increased SR-BI expression is associated with low HDL-C and reduced atherosclerosis (30−36). Although considerable risk could be associated with injecting even small amounts of rSOF, improvement of multiple steps in RCT by rSOF in cellular and animal models of atherosclerosis would provide a compelling rationale for developing alternative therapeutically appropriate opacification methods.

REFERENCES

1. Havel, RJ.; Goldstein, JL.; Brown, MS. Lipoproteins in Lipid Transport. In: Bondy, PK.; Rosenberg, LE., editors. The Metabolic Control of Disease. 1980. p. 398-494.
2. Gotto, AM.; Pownall, HJ, Jr. Manual of Lipid Disorders. 3rd ed. Baltimore, MD: Lippincott Williams and Wilkins; 2003. p. 462

3. Gotto, AM.; Pownall, HJ.; Havel, RJ, Jr. Plasma Lipoproteins. In: Segrest, J.; Albers, J., editors. Methods in Enzymology. Vol. Vol. 128. 1986. p. 3-41.
4. Massey JB, Hickson D, She HS, Sparrow JT, Via DP, Gotto AM, Pownall HJ Jr. Measurement and prediction of the rates of spontaneous transfer of phospholipids between plasma lipoproteins. Biochim. Biophys. Acta 1984;794:274–280. [PubMed: 6733137]
5. Tall A. Plasma lipid transfer proteins. Annu. Rev. Biochem 1995;64:235–257. [PubMed: 7574481]
6. Reijngoud D-J, Phillips MC. Mechanism of dissociation of human apolipoprotein A-I, A-II, and C from complexes of dimyristoylphosphatidylcholine as studied by thermal denaturation. Biochemistry 1984;23:726–734.
7. Mehta R, Gantz DL, Gursky O. Human plasma high-density lipoproteins are stabilized by kinetic factors. J. Mol. Biol 2003;328:183–192. [PubMed: 12684007]
8. Pownall HJ. Remodeling of human plasma lipoproteins by detergent perturbation. Biochemistry 2005;44:9714–9722. [PubMed: 16008356]
9. Sparks DL, Phillips MC, Lund-Katz S. The charge and structural stability of apolipoprotein A-I in discoidal and spherical recombinant high density lipoprotein particles. J. Biol. Chem 1992;267:25839–25847. [PubMed: 1464598]
10. Pownall HJ, Hosken BD, Gillard BK, Higgins CL, Lin HY, Massey JB. Speciation of human plasma high density lipoprotein: HDL stability and apolipoprotein A-I partitioning. Biochemistry 2007;46:7449–7459. [PubMed: 17530866]
11. Oram JF, Lawn RM, Garvin MR, Wade DP. ABCA1 is the cAMP-inducible apolipoprotein receptor that mediates cholesterol secretion from macrophages. J. Biol. Chem 2000;275:34508–34511. [PubMed: 10918070]
12. Acton S, Rigotti A, Landschulz KT, Xu S, Hobbs HH, Krieger M. Identification of scavenger receptor SR-BI as a high density lipoprotein receptor. Science 1996;271:518–520. [PubMed: 8560269]
13. Glass C, Pittman RC, Weinstein DB, Steinberg D. Dissociation of tissue uptake of cholesterol ester from that of apoprotein A-I of rat plasma high density lipoprotein: selective delivery of cholesterol ester to liver, adrenal, and gonad. Proc. Natl. Acad. Sci. U.S.A 1983;80:5435–5439. [PubMed: 6412229]
14. Courtney HS, Hasty DL, Li Y, Chiang HC, Thacker JL, Dale JB. Serum opacity factor is a major fibronectin-binding protein and a virulence determinant of M type 2 *Streptococcus pyogenes*. Mol. Microbiol 1999;32:89–98. [PubMed: 10216862]
15. Cunningham MW. Pathogenesis of group A streptococcal infections. Clin. Microbiol. Rev 2000;13:470–511. [PubMed: 10885988]
16. Courtney HS, Zhang YM, Frank MW, Rock CO. Serum opacity factor, a streptococcal virulence factor that binds to apolipoproteins A-I and A-II and disrupts high density lipoprotein structure. J. Biol. Chem 2006;281:5515–5521. [PubMed: 16407233]
17. Pownall HJ. Detergent-mediated phospholipidation of plasma lipoproteins increases HDL cholesterophilicity and cholesterol efflux via SR-BI. Biochemistry 2006;45:11514–11522. [PubMed: 16981711]
18. Hamilton JA, Miller KW, Small DM. Solubilization of triolein and cholesteryl oleate in egg phosphatidylcholine vesicles. J. Biol. Chem 1983;258:12821–12826. [PubMed: 6685124]
19. Tanford, C. The Hydrophobic Effect: Formation of Micelles and Biological Membranes. New York: Wiley-Interscience; 1980. p. 57
20. Rao R, Albers JJ, Wolfbauer G, Pownall HJ. Molecular and macromolecular specificity of human plasma phospholipid transfer protein. Biochemistry 1997;36:3645–3653. [PubMed: 9132017]
21. Lusa S, Jauhiainen M, Mets J, Somerharju P, Ehnholm C. The mechanism of human plasma phospholipid transfer protein-induced enlargement of high-density lipoprotein particles: evidence for particle fusion. Biochem. J 1996;313:275–282. [PubMed: 8546695]
22. Silver ET, Scraba DG, Ryan RO. Lipid transfer particle-induced transformation of human high density lipoprotein into apolipoprotein A-I-deficient low density particles. J. Biol. Chem 1990;265:22487–22492. [PubMed: 2125050]
23. Liang HQ, Rye KA, Barter PJ. Remodelling of reconstituted high density lipoproteins by lecithin:cholesterol acyltransferase. J. Lipid Res 1996;37:1962–1970. [PubMed: 8895062]

24. Rye KA, Hime NJ, Barter PJ. Evidence that cholesteryl ester transfer protein-mediated reductions in reconstituted high density lipoprotein size involve particle fusion. J. Biol. Chem 1997;272:3953–3960. [PubMed: 9020099]
25. Brinton EA, Eisenberg S, Breslow JL. Increased apo A-I and apo A-II fractional catabolic rate in patients with low high density lipoprotein-cholesterol levels with or without hypertriglyceridemia. J. Clin. Invest 1991;87:536–544. [PubMed: 1899429]
26. Vitello LB, Scanu AM. Studies on human serum high density lipoproteins. Self-association of apolipoprotein A-I in aqueous solutions. J. Biol. Chem 1976;251:1131–1136. [PubMed: 175065]
27. Swenson TL, Brocia RW, Tall AR. Plasma cholesteryl ester transfer protein has binding sites for neutral lipids and phospholipids. J. Biol. Chem 1988;263:5150–5157. [PubMed: 2833496]
28. Wetterau JR, Lin MC, Jamil H. Microsomal triglyceride transfer protein. Biochim. Biophys. Acta 1997;1345:136–150. [PubMed: 9106493]
29. Swift LL, Kakkad B, Boone C, Jovanovska A, Jerome WG, Mohler PJ, Ong DE. Microsomal triglyceride transfer protein expression in adipocytes: a new component in fat metabolism. FEBS Lett 2005;579:3183–3189. [PubMed: 15922333]
30. Varban ML, Rinninger F, Wang N, Fairchild-Huntress V, Dunmore JH, Fang Q, Gosselin ML, Dixon KL, Deeds JD, Acton SL, Tall AR, Huszar D. Targeted mutation reveals a central role for SR-BI in hepatic selective uptake of high density lipoprotein cholesterol. Proc. Natl Acad. Sci. U.S.A 1998;95:4619–4624. [PubMed: 9539787]
31. Kozarsky KF, Donahee MH, Rigotti A, Iqbal SN, Edelman ER, Krieger M. Overexpression of the HDL receptor SR-BI alters plasma HDL and bile cholesterol levels. Nature 1997;387:414–417. [PubMed: 9163428]
32. Trigatti B, Rayburn H, Vinals M, Braun A, Miettinen H, Penman M, Hertz M, Schrenzel M, Amigo L, Rigotti A, Krieger M. Influence of the high density lipoprotein receptor SR-BI on reproductive and cardiovascular pathophysiology. Proc. Natl. Acad. Sci. U.S.A 1999;96:9322–9327. [PubMed: 10430941]
33. Braun A, Trigatti BL, Post MJ, Sato K, Simons M, Edelberg JM, Rosenberg RD, Schrenzel M, Krieger M. Loss of SR-BI expression leads to the early onset of occlusive atherosclerotic coronary artery disease, spontaneous myocardial infarctions, severe cardiac dysfunction, and premature death in apolipoprotein E-deficient mice. Circ. Res 2002;90:270–276. [PubMed: 11861414]
34. Covey SD, Krieger M, Wang W, Penman M, Trigatti BL. Scavenger receptor class B type I-mediated protection against atherosclerosis in LDL receptor-negative mice involves its expression in bone marrow-derived cells. Arterioscler., Thromb., Vasc. Biol 2003;23:1589–1594. [PubMed: 12829524]
35. Arai T, Wang N, Bezouevski M, Welch C, Tall AR. Decreased atherosclerosis in heterozygous low density lipoprotein receptor-deficient mice expressing the scavenger receptor BI transgene. J. Biol. Chem 1999;274:2366–2371. [PubMed: 9891004]
36. Ueda Y, Gong E, Royer L, Cooper PN, Francone OL, Rubin EM. Relationship between expression levels and atherogenesis in scavenger receptor class B, type I transgenics. J. Biol. Chem 2000;275:20368–20373. [PubMed: 10751392]

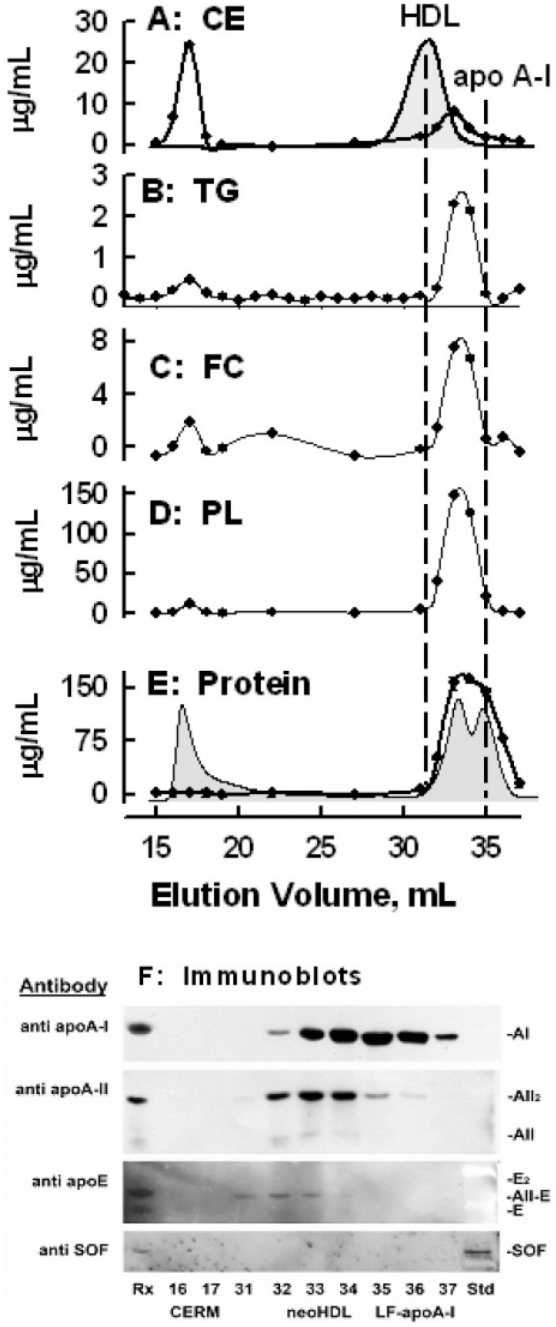

FIGURE 1.

Redistribution of 0.5 mg/mL HDL components by rSOF according to SEC. Human HDL (0.5 mg/mL) was incubated with rSOF (1 µg/mL) at 37 °C for 24 h. The absorbance profile for HDL is shown as the filled curve in A. The products were separated by SEC and the collected fractions analyzed for cholesteryl ester (CE), triglyceride (TG), free cholesterol (FC), and phospholipid (PL) (A–D, respectively); E, absorbance (280 nm) of the column effluent (filled curve) and total protein according to direct analysis of collected fractions (●). F: Immunoblot analysis of collected fractions as labeled. Rx: Aliquot of reaction mixture. Std: 10 ng of rSOF and Kaleidoscope molecular weight standards (BioRad).

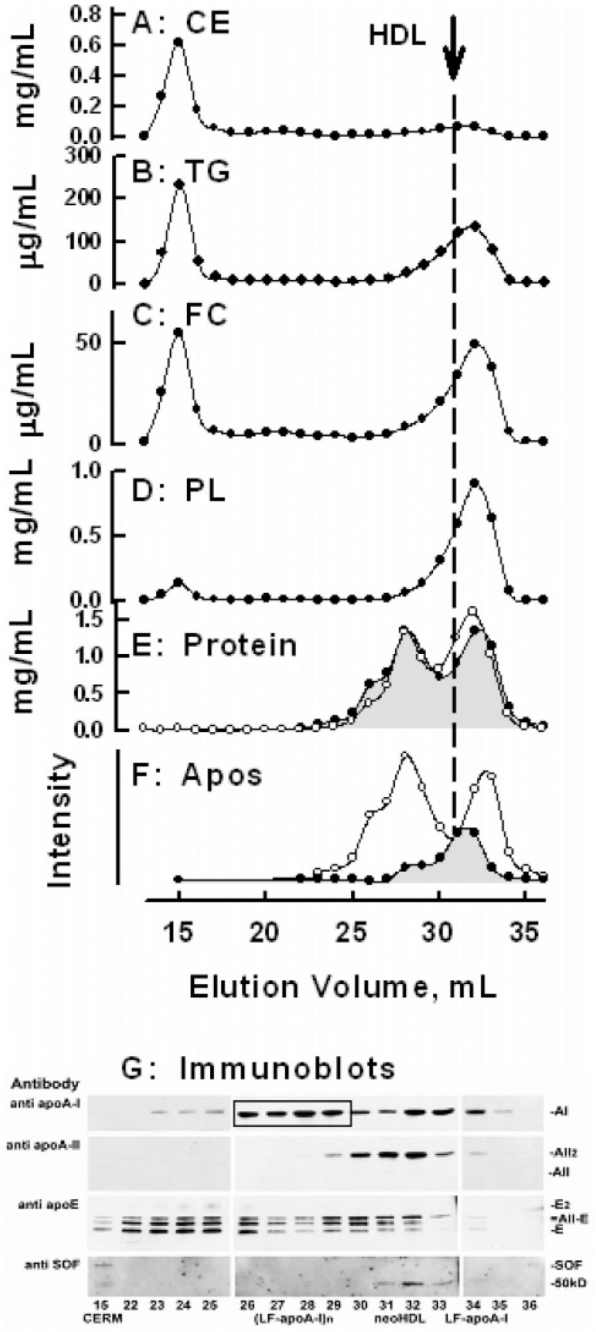

FIGURE 2.

Redistribution of 21 mg/mL HDL components by rSOF according to SEC. Whole human HDL (21 mg/mL) was incubated with rSOF (4 μg/mL) at 37 °C for 24 h. See Figure 1A–D for details. E: Total protein according to direct analysis (○) and relative protein content according to quantitative densitometric immunoblotting of SDS–PAGE (●, gray fill). F: Apo A-I (○) and apo A-II (●, gray fill) according to immunoblot densitometry. G: Immunoblot analysis of collected fractions as labeled. The relative amounts loaded per lane were 20 μL (fraction 15), 10 μL (fractions 22–25 and 34–36), and 3 μL (fractions 26–33).

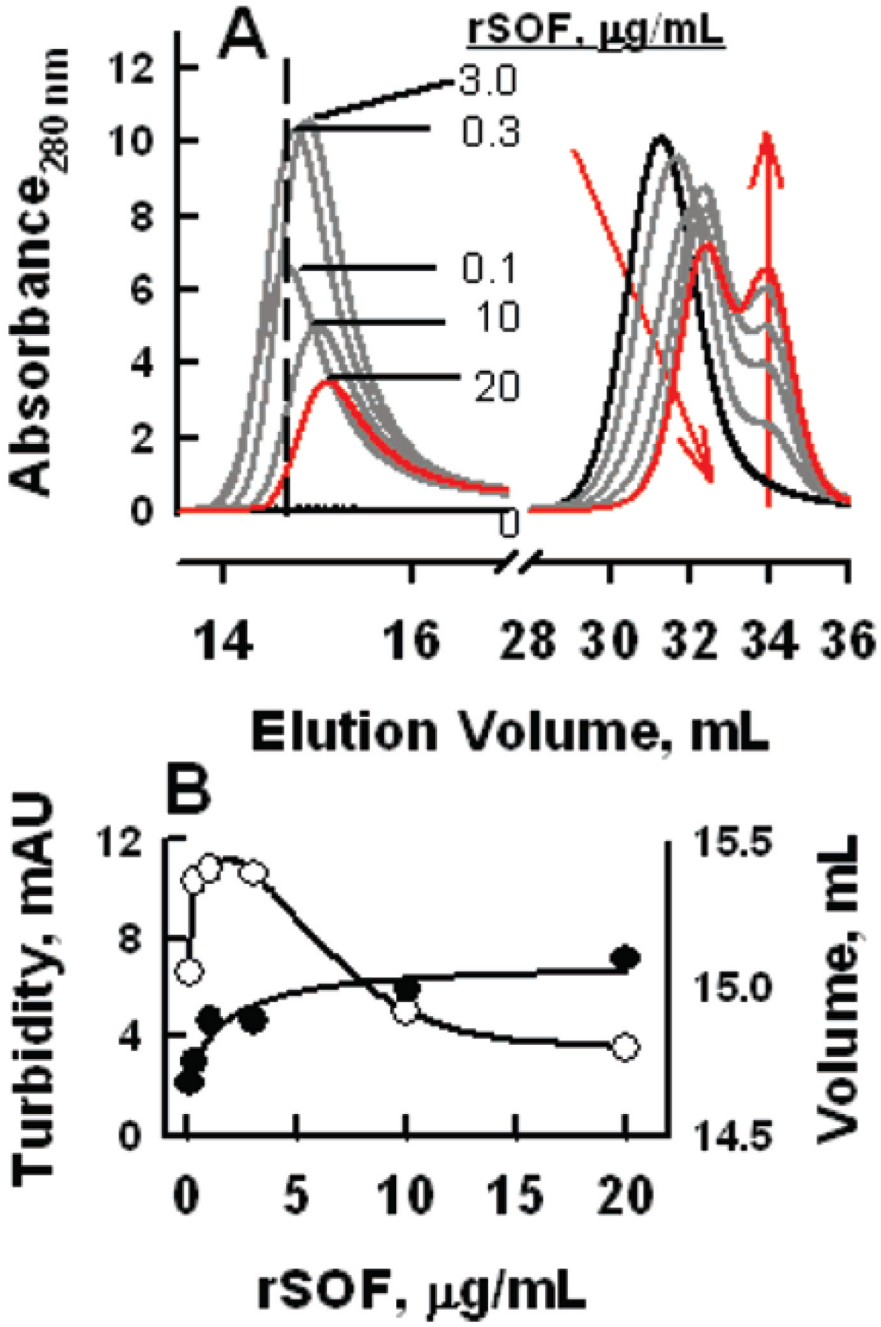

FIGURE 3.

Effect of rSOF concentration. A: HDL (0.25 mg/mL) was incubated with various concentrations of rSOF for 0.5 h at 37 °C, quenched by immersion in ice for ~10 min, and analyzed by SEC. HDL profile in the absence of rSOF (—). rSOF concentrations are indicated with the profile at the highest concentration (20 μg/mL) shown by a red line. The dashed vertical line denotes the void volume. The red arrows indicate the direction of the shift in the SEC profiles with increasing rSOF. B: CERM turbidity (○; splined, smoothed curve) and peak elution volume (●; hyperbolic 3-parameter fit) as a function of rSOF concentration.

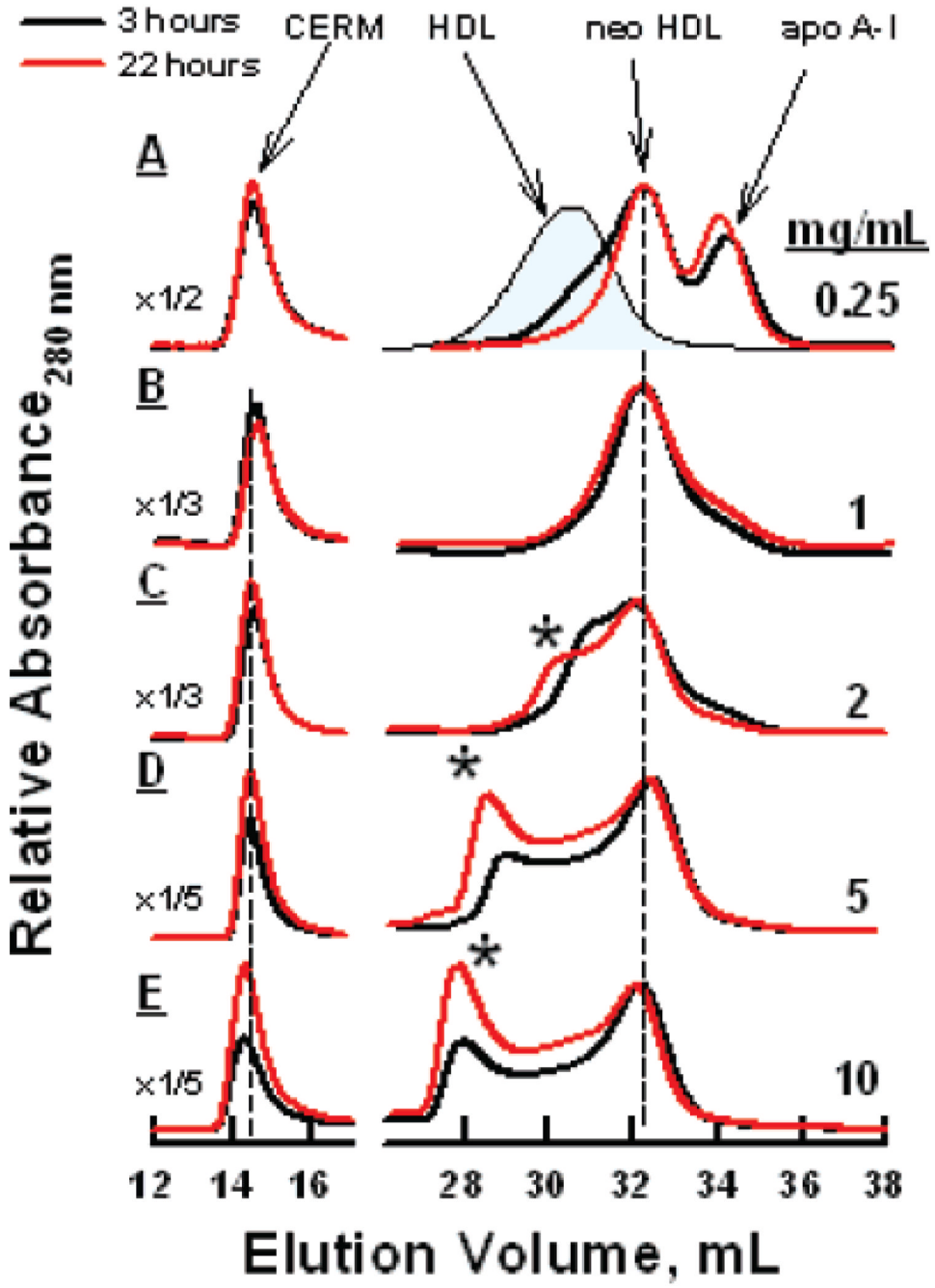

FIGURE 4.

Effect of HDL concentration on rSOF activity. Various concentrations of HDL in 1 mL were combined with 4 μg of rSOF and incubated at 37 °C for 3 (—) and 22 h (red line) and analyzed by SEC. Panels A–E are the SEC of HDL at 0.25, 1, 2, 5, and 10 mg/mL HDL-protein, respectively. The gray-filled curve in A is the SEC profile for HDL without incubation with rSOF. The absorbance due to light scattering in the void volume (peak elution ~14 mL) is much greater than that of the protein absorbance in the right-hand panel; thus, the absorbances in the left-hand panels have been multiplied by the fractions as shown. Asterisks denote the peaks for apo A-I oligomers.

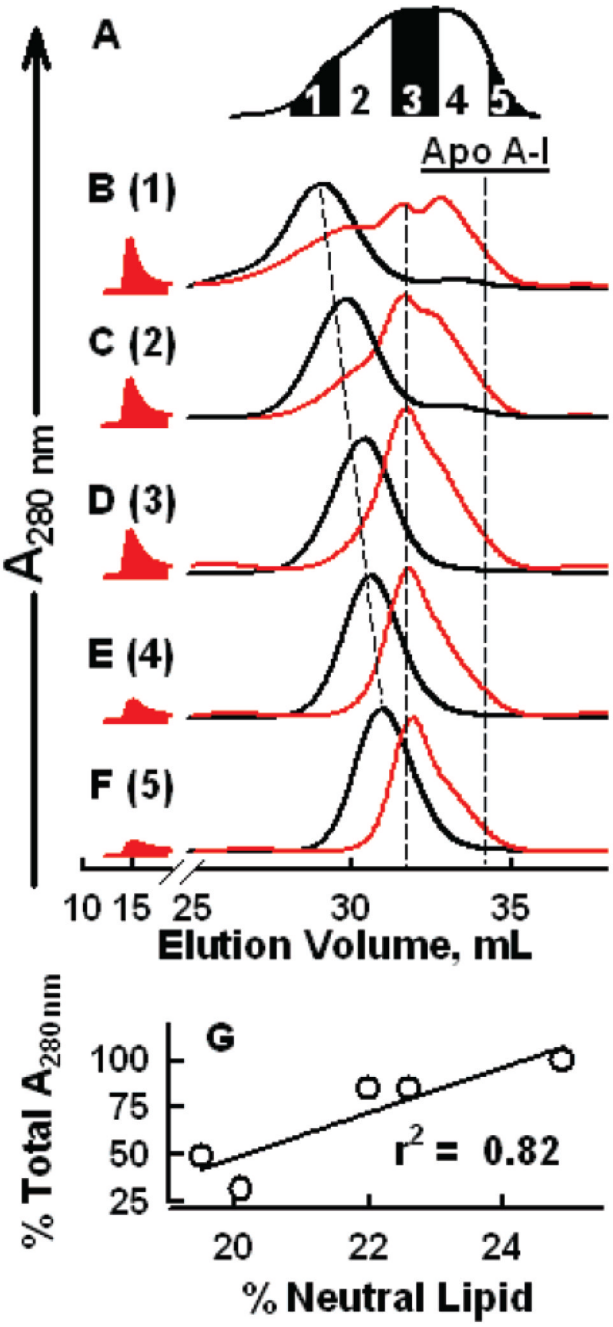

FIGURE 5.

Effects of rSOF on HDL subfractionated according to size. A: Fractionation of HDL by SEC. B–F: SEC analysis of HDL subfractions (1.2 mg/mL) from A before (—) and after (red line) 24 h of incubation with rSOF (1.1 μg/mL) at 37 °C. Relative to fraction 1 = 100%), the peak heights for the void volumes were 85, 85, 49, and 32% for fractions 2−5, respectively. G: Void volume peak area (red filled) as a function of neutral lipid content (CE + TG; Table 2) of the starting HDL subfractions.

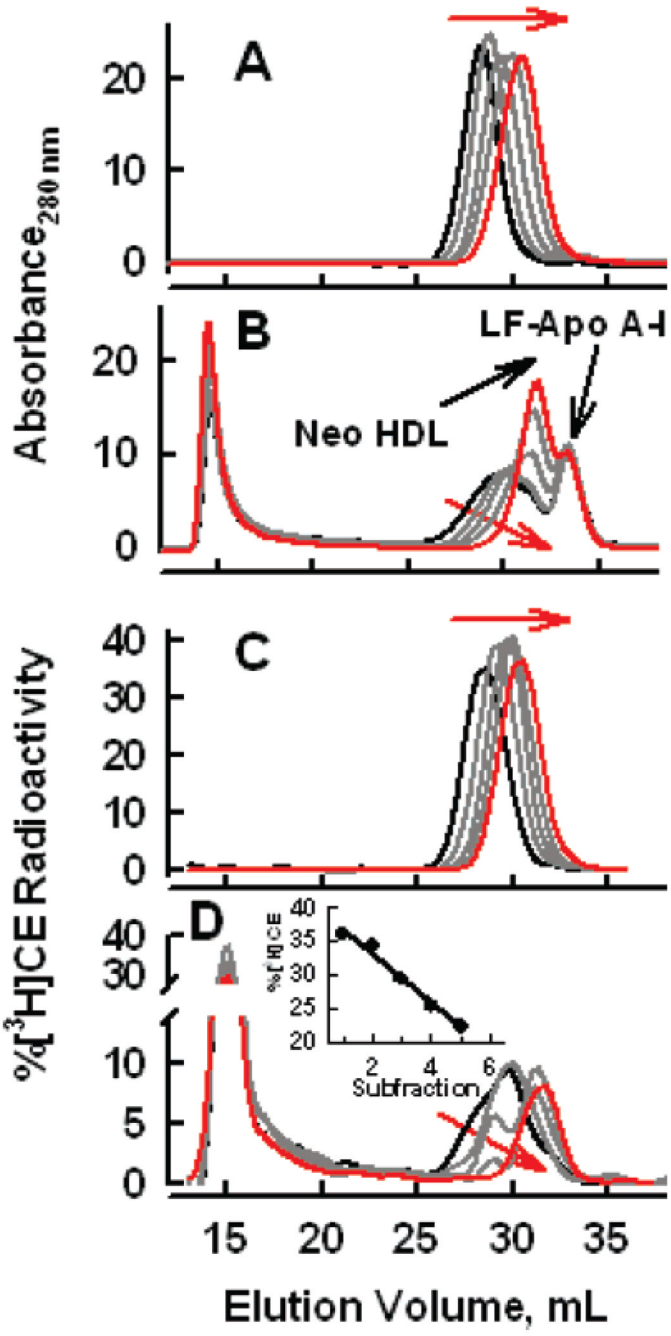

FIGURE 6.

Effect of rSOF on SEC profiles of [^{3}H]CE-labeled HDL subfractions. HDL (0.5 mg/mL) and rSOF (1 μg/mL) were incubated at 37 °C for 3 h and analyzed by SEC. Elution profiles are shown for absorbance at 280 nm (A and B) and radioactivity (C and D). A, C) SEC profiles of HDL subfractions isolated by SEC. (B and D) SEC analysis of HDL after incubation with rSOF. In each panel, the largest and smallest HDL subfraction appear as black and red curves, respectively. Red arrows point in the direction of decreasing size. Peaks for neo HDL and LF-apo A-I are as indicated by black arrows. (D, insert) %[^{3}H]CE in neo HDL with decreasing size of the starting HDL (5 is the smallest). Line of regression includes all data ($r^2 > 0.98$).

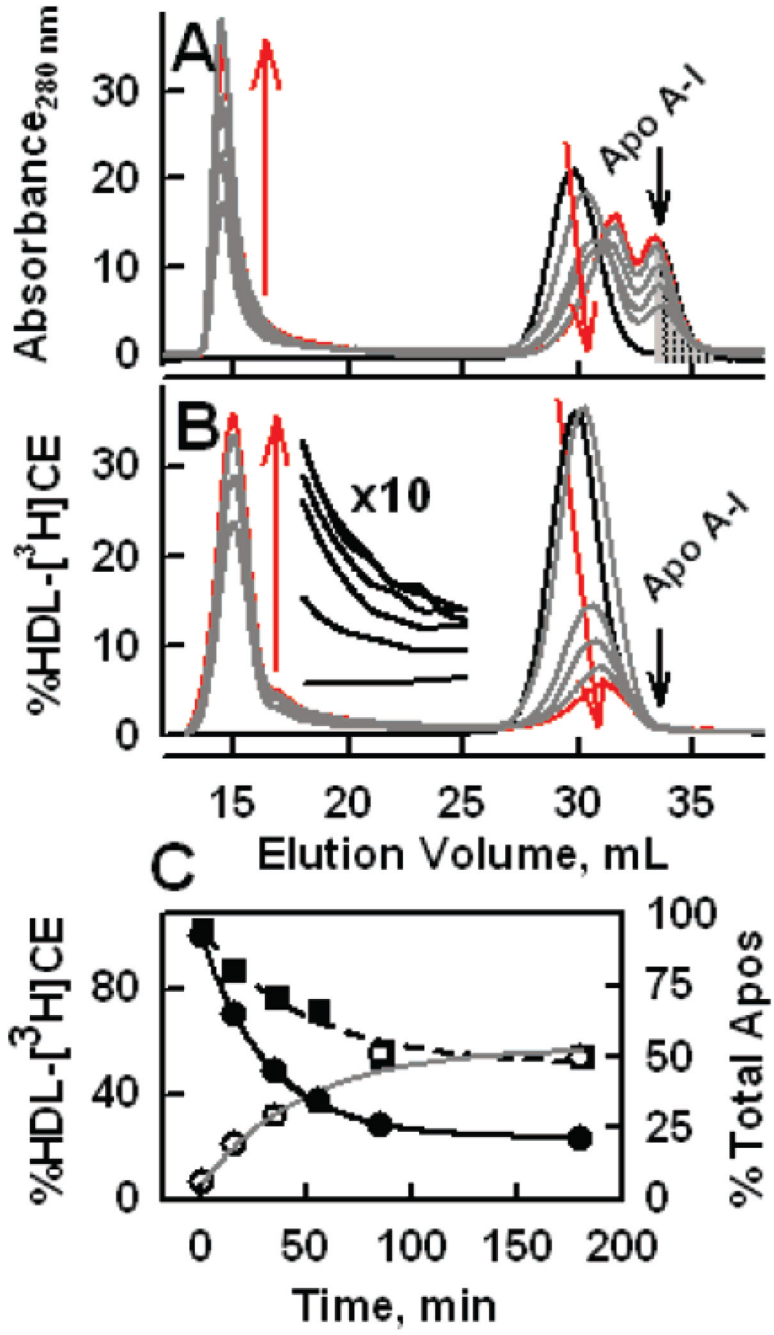

FIGURE 7.

Kinetics of rSOF-catalyzed HDL opacification. HDL-[^{3}H]CE (0.5 mg/mL) was incubated with rSOF (1 μg/mL) at 37 °C for various times as labeled, cooled with wet ice, and analyzed by SEC in which the effluent was monitored by absorbance at 280 nm (A) and by the radioactivity (B) of the collected fractions; curves for 0 and 180 min are black and red, respectively. The red arrows indicate the shift in the adjacent profiles with time = 0, 15, 35, 55, 85, 180 min. A, absorbance; B, radioactivity; insert, the radioactivity multiplied by 10. C, kinetics of the appearance of LF-apo A-I calculated as twice the percent of total protein absorbance in the double shaded portion in A (○); kinetics of the disappearance of HDL calculated from the total protein absorbance minus absorbance due to LF-apo A-I (■); kinetics of the disappearance of

HDL-associated [^{3}H]CE (●). On the basis of the disappearance of HDL-[^{3}H]CE and protein absorbance, respectively, $k_{CERM} = (3.2 \pm 0.008) \times 10^{-2}$ ($r^2 > 0.99$), and $k_{AI} = (2.1 \pm 0.006) \times 10^{-2}$ min^{-1} ($r^2 > 0.96$).

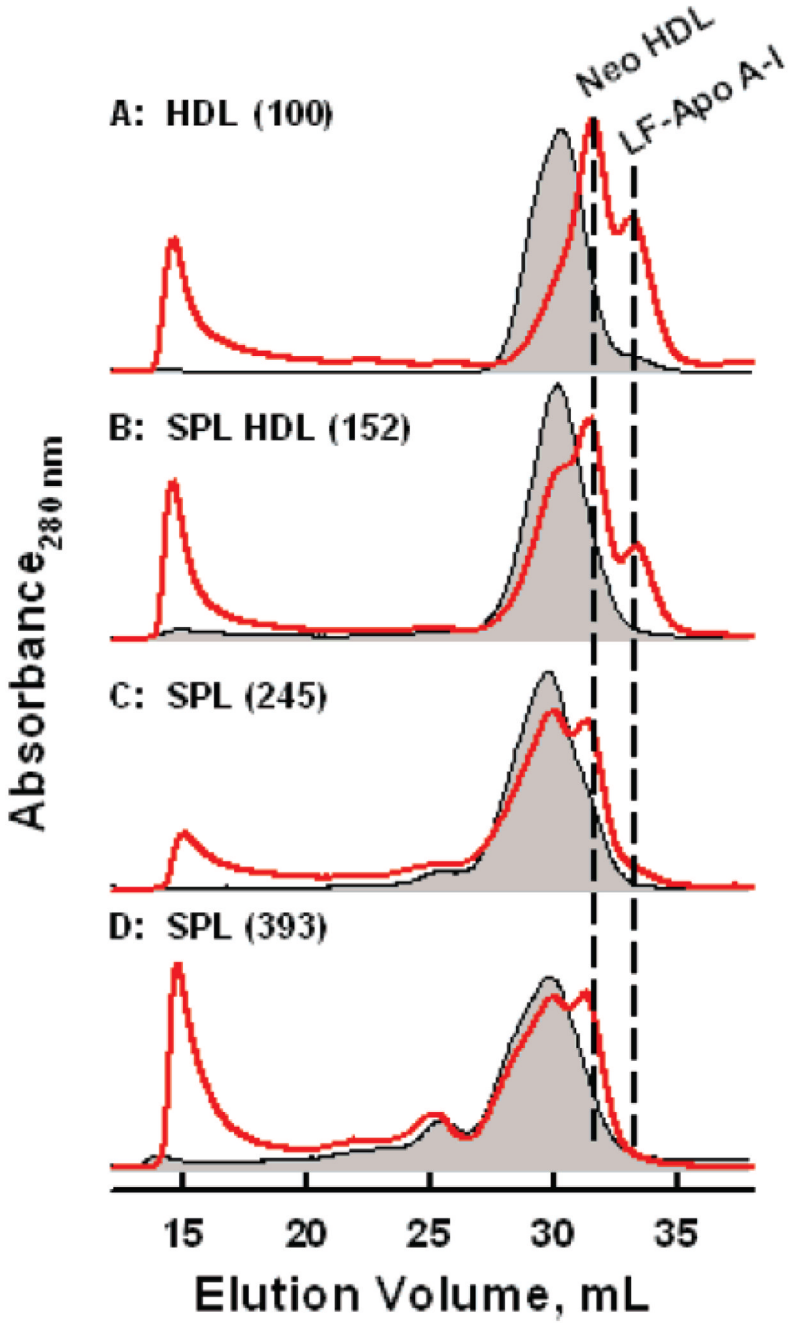

FIGURE 8.

Effect of superphospholipidation on HDL opacification by rSOF. Sodium cholate and POPC were combined in TBS to give final concentrations of 52.6 and 26.3 mM, respectively. Different amounts of cholate/POPC solution were added to HDL (1.3 mg/mL) with rapid stirring. The final concentration in the mixture did not exceed the critical micelle concentration of sodium cholate (~15 mM). The SPLd HDL (1 mg/mL) were exhaustively dialyzed against TBS and reacted with rSOF (1 μg/mL). The SEC profiles are before (gray filled curve) and after (red line) incubation with rSOF. A, control HDL; B–D, SPLd HDL containing increasing amounts of PL as labeled. The vertical lines locate neo HDL and LF-apo A-I.

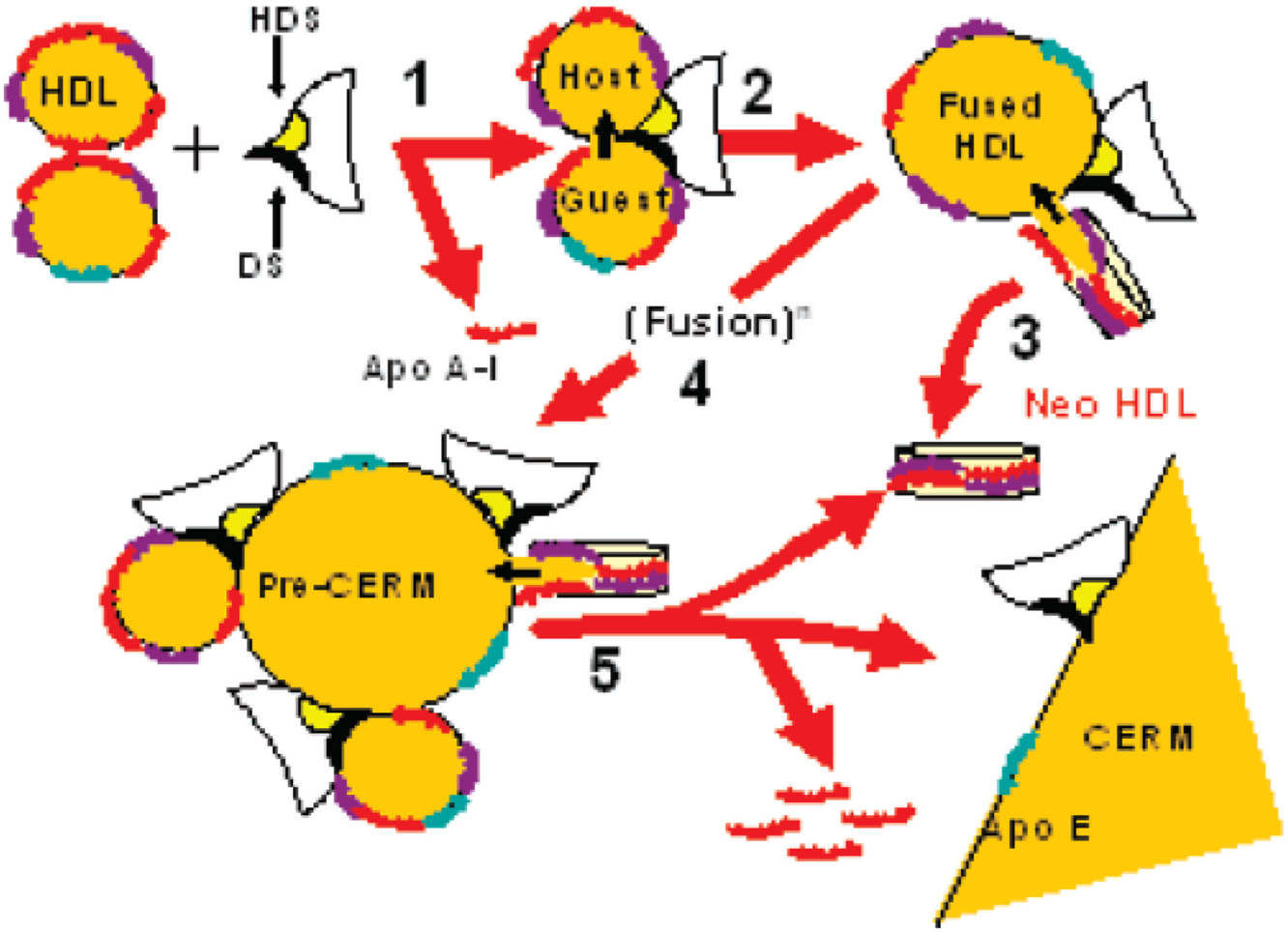

FIGURE 9.

Mechanistic model for rSOF-mediated opacification of HDL. Step 1: rSOF binds to HDL via its high affinity docking site (HDS) and its delipidation site (DS) while displacing apo A-I (red helix) from the HDL surface of both particles, thereby exposing the underlying CE. Step 2: contact between the exposed CE of tethered HDL particles forms a continuous CE stalk through which CE in the guest HDL transfers to and coalesces with that of the host HDL. Step 3: extrusion of the delipidated guest HDL produces apo A-II-rich (purple helix) neo HDL, which desorbs from the pre-CERM. Step 4: multiple cycles of HDL recruitment and delipidation form a pre-CERM that in step 5 grows into the mature CERM that contains surface-associated PL (not shown), apo E (green helix), and mostly CE. The CERM is presented as a partial structure of a very large particle, the surface of which appears flat when depicted on the same scale as that of HDL.

Table 1

Compositions of Products Formed from rSOF at High and Low HDL Concentrations[a]

	low concentration of HDL (0.5 mg/mL)							
	analytes (% composition)					(NL/particle)/(PL/particle)		
fraction	**PL**	**FC**	**CE**	**TG**	**protein**	**CE/PL**	**TG/PL**	**NL/PL (M/M)**
HDL	26.2	2.5	19.8	4.2	47.3	38/44 = 0.86	6/44 = 0.14	1.00
CERM	19.5	3.1	65.8	7.9	3.7	3.9	0.34	4.24
neo HDL	40.8	2.1	2.9	6.6	48.0	4/44 = 0.09	6/44 = 0.14	0.23
	high concentration HDL (21 mg/mL)							
HDL	24.4	3.0	17.3	4.4	51.0	33/41 = 0.80	6/41 = 0.15	1.05
CERM	12.4	5.2	58.0	21.9	2.5	5.4	1.5	6.9
(apo A-I)$_n$	4.3	0.6	1.8	1.8	91.4	n. d.	n. d.	n. d.
neo HDL	32.6	1.8	2.2	4.8	58.5	3/35 = 0.08	4/35 = 0.11	0.20

[a] Assumes that CE = 650 Da, TG = 885 Da, PL = 750 Da, HDL = 125 kDa, and neo HDL = 80 kDa. NL = CE + TG; n. d., not determined.

Table 2

Composition of HDL and Its Subfractions Separated by Size[a]

	%PL	%FC	%CE	%TG	%protein
total HDL	24.4 ± 1.2	2.95 ± 0.26	17.3 ± 1.0	4.42 ± 0.31	51.0 ± 5.5
1	29.8 ± 1.0	2.63 ± 0.08	21.2 ± 1.1	3.70 ± 0.26	42.7 ± 2.7
2	26.8 ± 4.2	2.39 ± 0.11	19.3 ± 0.9	3.28 ± 0.14	48.2 ± 2.2
3	28.9 ± 0.7	2.12 ± 0.21	19.0 ± 0.3	3.04 ± 0.08	46.9 ± 0.6
4	27.0 ± 1.2	1.92 ± 0.15	16.8 ± 0.5	2.65 ± 0.10	51.7 ± 2.7
5	25.8 ± 1.1	1.81 ± 0.09	17.4 ± 1.3	2.73 ± 0.09	52.3 ± 2.1

[a]The HDL subfractions correspond to fractions 1–5 of Figure 5.